OPTIMAL DESIGN OF A STIFFENED PLATE SUBJECTED TO COMBINED LONGITUDINAL AND LATERAL LOADS

Y.C. Huang,
Centre for Marine Engineering and Ocean Technology (CENTEC), Instituto Superior Técnico, Universidade de Lisboa, Lisbon, 1049-001 Portugal

ABSTRACT: This paper is to design and optimise a stiffened plate which serves as a part of a ship structure. Multi-Objective structural optimization of a stiffened plate subjected to a combined stochastic buckling and fatigue loads in minimising the structural section area, the maximum displacement and fatigue damage satisfying a predefined target reliability level is performed. The Pareto frontier solutions calculated by Non-Dominated Sorting Genetic Algorithm (NSGA-II) were used to define the feasible surface of the design variables. The first order reliability method is employed to identify the topology of the stiffened plate as a part of the Pareto frontier solutions in reducing the failure probability due to fatigue and buckling. Comparing with the original section area, the optimised section area decreased by 8%.

1 INTRODUCTION

Steel stiffened panels are mainly used for the structural design of ships. They are usually used in ship and ocean structures to withstand tensile or compressive axial load and lateral pressure, due to the effect of waves and hydrostatic pressure in the ocean. For the safety of ship structure, it is critical to predicting its load carrying capacity. Under complex bending conditions, the effect of lateral pressure on the plate collapse strength of the plate depends on the interaction of axial and lateral loads [1]. The Pareto frontier, ultimate limit state, and target reliability, defined as additional constraints to determine the optimal design solution as demonstrated in [2].

Limit state method has been widely applied in ship design, presented by IACS, Common Structural Rules for Bulk Carriers and Oil Tankers [3]. Recent developments in structural reliability methods and optimisation tools allow design methods based on coupling the reliability analysis, in which the uncertainties related to design variables can be considered directly.

The FORM (first order reliability methods) approaches have been used for structural assessment as shown in [4-7], but it can also be used for probabilistic analysis of different practical applications [8].

The reliability analysis performed in this paper is FORM, which provides a method for evaluating reliability with reasonable accuracy and is sufficient for practical application.

Combining the reliability methods with the structural optimisation techniques, the three-step method of stiffened panel design is proposed. Once the structure topology is determined, the scantling of the structural components of the stiffened plate is performed and optimized, in which the design variables and the objective functions related to the minimum net section area, which satisfied the minimum weight, displacement fatigue damage and constraints requirements, including the ultimate compressive strength are defined in a purely deterministic manner.

Then the Pareto frontier method [9] is used to determine the optimal design solution, which satisfies all the constraints and minimises the three objective functions. The results can be used as a basis for the target reliability-based optimisation, which is required to guarantee the structural integrity. This step accommodates the uncertainties of the design variables, and the computational models are involved.

The primary objective is to optimise the dimensions of a stiffened plate of a ship. The calculation of some primary input data such as loads on the ship is based on empirical formulas and specification rules, not on actual records of sea state conditions. It is optimised without specific and detailed data from a ship, so the classical method is not applicable here because it is difficult to give criteria to determine whether the feasible solution is retained or not.

The objective is to perform a multi-objective optimisation of ship stiffened plates and to obtain a complete method flow suitable for solving this kind of problems of various ships at the same time. In this paper, the author chooses NSGA-II [9]to ensure that the optimal solution can be obtained quickly with sufficient quantity and accuracy when only the ship's main dimensions are known.

The Pareto frontier is applied for simultaneous minimisation of the net sectional area, structural displacement and fatigue damage.

Employing the Pareto Frontier, an optimal solution, accounting for the existing constraints, may be chosen using a utility function to rank the different designs, or by using 2D or 3D scatter diagrams to identify the more attractive ones. In the present study, an additional constraint is introduced representing the target reliability level to determine the most appropriate design solution.

2 ULTIMATE STRENGTH OF SHI HULL

2.1 *Main dimension of bulk carrier*

A 175,000-ton bulk carrier is used as a target ship. The main dimensions of the bulk carrier are:

- Length between the perpendiculars: L = 289 m;
- Depth: D = 24.7 m;
- Breadth: B = 45 m;
- Design Draft: d = 18 m;
- Block Coefficient: C_b = 0.79.

Half cross-section of the hull girder of this bulk carrier is shown in Figure 1. The cross-section contains a total of 129 plates and 98 stiffeners. A longitudinal stiffened plate of a tee-bar profile, with a stiffener spacing of 860 mm and a frame span of 2,950 mm, is analysed in the present study.

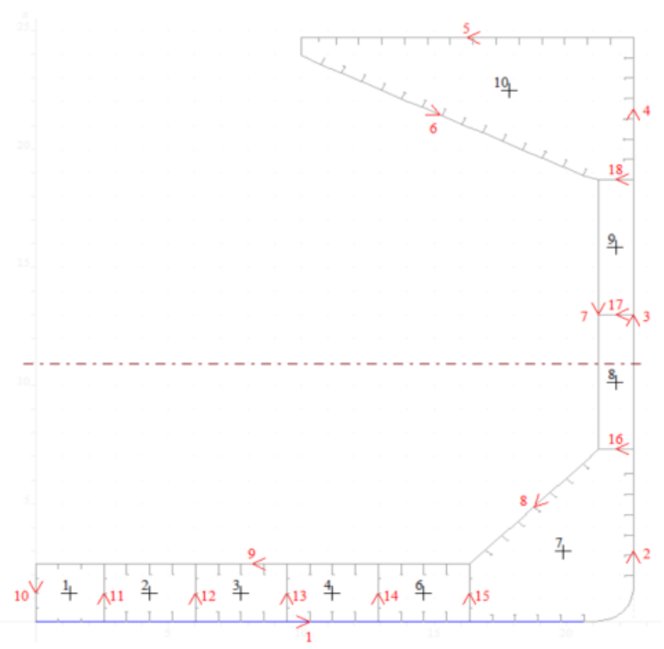

Figure 1 Half cross section of a bulk carrier

Considering the geometrical characteristics of the bulk carrier, the plates and stiffeners of the midship section are shown in Figure 1. The details of the longitudinal stiffeners are summarised in Table 1, and the material properties are listed in Table 2 respectively.

Table 1 Dimensions of longitudinals

No.	Dimensions (mm)	Type	Y.S.(MPa)
1	200 × 20	Flat bar	320
2	150 × 18	Flat bar	320
3	250 × 25	Flat bar	320
4	200 × 20	Flat bar	320
5	420 × 12 + 100 × 20	Tee-bar	320
6	420 × 12 + 100 × 30	Tee-bar	320
7	320 × 12 + 100 × 18	Tee-bar	320
8	300 × 12 + 100 × 12	Tee-bar	320
9	300 × 12 + 100 × 16	Tee-bar	320
10	350 × 12 + 100 × 20	Tee-bar	360
11	300 × 12 + 100 × 18	Tee-bar	360
12	300 × 30	Flat bar	360
13	200 × 20	Flat bar	360
14	350 × 30	Flat bar	360
15	300 × 12 + 100 × 24	Tee-bar	360

Table 2 Material properties

	1	2	3
Young's modulus(N/mm^2)	2,1E5	2.1E5	2.1E5
Poisson ratio	0.3	0.3	0.3
Yielding stress (N/mm^2)	235	320	360

2.2 *Ultimate strength of ship hull*

The software MARS2000 [10] is used to estimate the ultimate strength and geometrical descriptors of the midship section. Once the midship section is designed, which includes the position, shape and properties of all plates and stiffeners, the features, of the hull girder are estimated and shown in Figure 2.

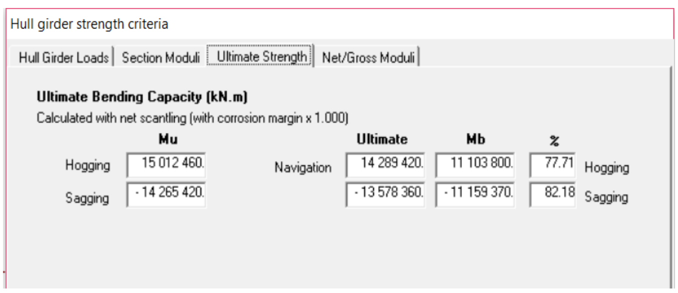

Figure 2 Ultimate strength of ship hull

3 BOTTOM STIFFENED PLATE

3.1 *Descriptors of stiffened plate*

For bulk carriers in hogging, the most critical loading is the alternate hold loading (AHL) condition with odd-numbered holds loaded with high-density cargoes and even numbered holds empty. The effect of the local lateral pressure should be considered in the assessment of the ultimate hull girder strength in the hogging and AHL conditions. In the present study, the ultimate strength of a bulk carrier hull girder under combined global and local loads in the hogging and AHL condition is investigated following the guidelines presented in [11].

The position of the stiffened plate selected for optimisation is on the bottom plate of the ship, which has coordinates of the weld position of the specified stiffener as (3.44, 0). The transverse distance from the middle of the ship is 3.44 m, and the height is 0 m. The stiffener type at this position is T-bar. The thickness of its adjacent bottom plates is 18 mm on both sides of it. The original geometric parameters of the stiffened plate are shown in Table 3. The geometry parameters of the specific plate are shown in Figure 3.

Table 3 Original geometric parameters of the stiffened plate

Width of bottom plate, s	860mm
Web height, h_w	420mm
Web thickness, t_w	12mm
Flange Breadth, b_f	100mm
Flange thickness, t_f	20mm

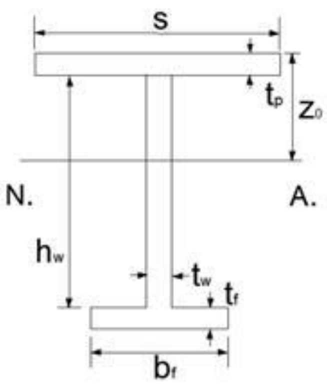

Figure 3 T-type stiffened plate cross-section

3.2 *Loads of stiffened plate*

The wave-induced bending moments in hogging and sagging as given by DNV Rules are used here. The wave-induced bending moments in hogging and sagging conditions are estimated and in the case in the case of hogging: $M_{w,h}^{CSR} = 6{,}043{,}951$ kNm, and in the case of sagging: $M_{w,s}^{CSR} = -6{,}599{,}624$ kNm.

The still water bending moments in hogging and sagging conditions are estimated as $M_{sw,h}^{CSR} = 4{,}455{,}451$ kNm and $M_{sw,s}^{CSR} = -3{,}899{,}778$ kNm.

The local static and dynamic pressure loads in full load condition is defined as $\mathrm{P_{sw}^{CSR}} = \rho g \mathrm{T_{LCi}} = 180\mathrm{Pa}$ and $\mathrm{P_W^{CSR}} = 3 f_P f_{nl} C \sqrt{,(1)\frac{L+\text{-}125}{L}} \left(\frac{z}{T_{LCi}} + \frac{|2y|}{B_i} + 1\right) = 46.94\mathrm{kPa}$ and in the ballast load condition as $P_W^{CSR} = 44$ kPa.). The inertia moment of the midship net section with respect to the neutral axis is $I_{na} = 603.2\ \mathrm{m}^4$.

Moreover, the midship section modulus concerning the bottom line is $W_b = 55.3\ \mathrm{m}^3$. The yield strength is $\sigma_y = 315$ MPa and the Young modulus is $E = 210$ GPa.

The geometry parameters as presented in Table 3 will be redefined during the optimisation process. The studied longitudinal stiffener is subjected to an axial load resulting from the vertical still water and wave-induced bending moments as:

$$\sigma_{global} = \frac{M_{sw} + \Psi M_w}{W_{bottom\ ship}} = 178{,}850\ \mathrm{kPa} \quad (2)$$

where Ψ is a combination factor between the still water and wave-induced loads ranging from 0.8 to 0.95 depending on the assumptions and it is assumed here to be a deterministic one of 0.9 [12]. The stiffener plate is also subjected to a lateral load, which is induced by the hydrostatic and dynamic local pressure. In the case of a full load condition:

$$q_{local1} = (P_{sw1} + \Psi P_{w1}) b_p = 191.9\ \mathrm{kN/m} \quad (3)$$

and in the case of the ballast load condition:

$$q_{local2} = (P_{sw2} + \Psi P_{w2}) b_p = 141.5\ \mathrm{kN/m} \quad (4)$$

The stiffened plate is assumed to be a simply supported beam subjected to a uniformly distributed lateral load, q_{local} and axial tensile force $\mathrm{T} = A(M_{sw,s} + \Psi M_{w,s})/W_{bottom\ ship}$ in the case of sagging loading and to an axial compressive force $\mathrm{T}^* = A(M_{sw,h} + \Psi M_{w,h})/W_{bottom\ ship}$ in the case of hogging respectively, where A is the net sectional area of the stiffened plate [2].

The maximum stresses at the middle of the beam are calculated as:

$$\sigma_{max,x=0} = \sigma_{local} + \sigma_{global} \quad (5)$$

where:

$$\sigma_{local}(P_{sw}, P_w) = \frac{m_{x=0}(u^*)}{W_{stiffened\ plate}} \quad (6)$$

$$\sigma_{global}(M_{sw,s}, M_{w,s}) = \frac{M_{sw,s} + \Psi M_{w,s}}{W_{bottom\ ship}} \quad (7)$$

3.3 *Optimisation considering weight and fatigue*

The goal of the structural design is to find the optimal dimensions for the three-dimensional structures. Usually, this is regarded as a single objective optimisation problem. However, many design problems are multistate, multispecific or need to optimise multiple objectives simultaneously. There may be trade-offs between goals, and improving one feature requires compromising another. The challenge is to identify solutions that are part of the Pareto optimal set design, where no further improvement can be achieved without degrading one of the others.

Pareto optimisation problems have been found in various research fields, and computational methods have been developed to identify the Pareto frontier.

3.3.1 *Decision variables*

In this study there are five decision variables considered that determine the shape of the cross-sectional area. Choosing the appropriate range of the decision variables is a fundamental issue. The appropriate range can make it easier to get results that meet the specific requirements in the subsequent Pareto frontier calculation.

The decision variables assumed here are:

$$x_1 = t_p,\; x_2 = h_w,\; x_3 = t_w, x_4 = b_f,\; x_5 = t_f \quad (8)$$

$$x = \{x\_1, x\_2, x\_3, x\_4, x\_5\}^{-1} x = \{x_1, x_2, x_3, x_4, x_5\}^{-1} \;\; x = \{x\_1, x\_2, x\_3, x\_4, x\_5\}^{-1} \quad (9)$$

Moreover, their range is defined as:

$$x_{i,min} \le x_i \le x_{i,max}, i \in [1,5] \;\; x = \{x\_1,\; x\_2,\; x\_3,\; x\_4,\; x\_5\}^{-1} \quad (10)$$

The original dimensions of the stiffened plate with its attached plate considered here is $t_p = 0.018\,m, b_f = 0.1\,m,\; t_f = 0.02\,m,\; h_w = 0.42\,m,$ $t_w = 0.012\,m$. Since the optimal design is based on this model, the dimensions of the decision variables will not change too much. So it can be used as a reference for the definition of the new ranges of the variables. Then after some trial operations, the final definitions of the variable ranges are as follows:

$$x_{1,min} = 0.012\,m,\; x_{1,max} = 0.03\text{ m} \quad (11)$$

$$x_{2,min} = 0.4\,m,\; x_{2,max} = 0.5\,m \quad (12)$$

$$x_{3,min} = 0.012\,m,\; x_{3,max} = 0.03\text{ m} \quad (13)$$

$$x_{4,min} = 0.1\,m,\; x_{4,max} = 0.2\,m \quad (14)$$

$$x_{5,min} = 0.012\,m,\; x_{5,max} = 0.03\text{ m} \quad (15)$$

The min range of decision variable = [0.012, 0.4, 0.012, 0.1, 0.012];

The max range of decision variable = [0.03, 0.5, 0.03, 0.2, 0.03].

3.3.2 *Objective functions*

Three critical factors need to be taken into consideration leading to three objective functions that need to be built. All of them need to meet the requirement of the Classification Society Rules.

The two-objective structural responses considered is minimising the weight, which leads to minimising of the net sectional area and minimising the structural displacement, which defines a multi-objective optimisation problem:

$$F_1 = \min\{z_{x=0}(b, x)\} \quad (16)$$

$$F_2 = \min\{A(b, x)\} \quad (17)$$

where $z_{x=0}(b,x)$ is the displacement at the middle of the span and $A(b,x)$ is the net-sectional area of the stiffened plate, $b = \{\sigma_y, E\}^{-1}$ is for the material properties. The third objective function is to minimizing the fatigue damage:

$$F_3 = min\{D_{x=0}(b, x)\} \quad (18)$$

3.3.3 *Constraints*

The dimensions of the flange, web and attached plate of the stiffened plate have to satisfy the following restrictions:

$$G_1: x_1 - \frac{b_p}{C}\sqrt{\frac{\sigma_y}{235}} \quad (19)$$

$$G_2: x_3 - \frac{h_w}{C_w}\sqrt{\frac{\sigma_y}{235}} > 0 \quad (20)$$

$$G_3: x_5 - \frac{b_f}{C_f}\sqrt{\frac{\sigma_y}{235}} > 0 \quad (21)$$

where b_p is the space defined as a distance between the longitudinal stiffeners, C=100, $C_w = 75,\; C_f = 12$.

The type of load on the stiffened plate will induce the plate buckling since the stiffener is subjected to a tensile load and the attached plate to a compressive load in bending. Some variables for the optimisation are listed in Table 4 and 5. In the fatigue damage calculation, the S-N curve D as suggested in [3] is used.

Table 4 Two loading conditions and fraction of time

Load Condition		Fraction of time
Full load	Sagging	0.5
Ballast	Hogging	0.35

Table 5 Weibull shape factor and the reference period of wave

$h_{Weibull}$	0.931	-
$T_{reference}$	1	year
T_{wave}	8	sec

3.4 *Optimisation considered reliability*

The empirical formula for the assessment of load carrying capacity of the stiffened panel would be more useful for the design [13] and for the reliability analysis of ship structure, although the factors of safety in association with uncertainties and deviations should be considered carefully [2]. The reliability analysis performed here is using the FORM techniques that identify a set of primary random variables, which influence the limit-state under consideration.

The limit-state function defines a failure surface when equals to 0, which is, in fact, an (n-1) dimensional surface in the space of n primary variables. The formation of RBDO is similar to the one of the optimisations where the objective limits state function, g (b, x) is minimised, and it is subject to constraints, where b is the vector of the deterministic design variables and x is the vector of the random variables. The limit state function here is defined as [2]:

$$g(b,x)=\sigma_u(b,x)-\sigma_{\max}(b,x) \tag{22}$$

where

$$\sigma_{\max}(b,x)=\sigma_{global,\max}(b,x)+\sigma_{local,\max}(b,x) \tag{23}$$

$$\sigma_{global,\max}(b,x)=k_1(X_{m,sw}M_{sw}+\Psi X_{m,w}M_w)/W_b \tag{24}$$

$$\sigma_{local,\max}(b,x)=k_2(X_{p,sw}P_{sw}+\Psi X_{p,w}P_w)l/W_{b,stiff} \tag{25}$$

This surface divides the primary variable space in a safe region, where $g(b,x)>0$ and an unsafe area where $g(b,x)<0$. The failure probability of a structural component concerning a single failure mode can formally be written as:

$$P_f=P[g(b,x)\le 0]P_f=P[g(b,x)\le 0] \tag{26}$$

where P_f denotes the probability of failure. In practical applications, the FORM methods provide a way of evaluating the reliability efficiently with reasonably good accuracy [2].

The required safety index is defined here as β_{target}, the Beta indexes of all feasible design solution, which based on the sets of section sizes corresponding to the Pareto frontier solutions, are compared to the required target safety index, where the $\min\{\beta_{target}-\beta_i\}$ is the best reliability based design solution.

Seven deterministic variables are considered here as $b_1=t_p$, $b_2=h_w$, $b_3=t_w$, $b_4=b_f$, $b_5=t_f$, $b_6=\sigma_y$, $b_7=E$, and ten random variables $x_1=M_{w,BL,hog}$, $x_2=P_{w,BL,h}$, $x_3=M_{sw,BL,h}$, $x_4=P_{sw,BL,h}$, $x_5=\sigma_u$, $x_6=X_u$, $x_7=X_{p,sw}$, $x_8=X_{m,sw}$, $x_9=X_{p,w}$, $x_{10}=X_{m,w}$, are considered here.

The local lateral load is defined as $q_{local}=(X_{p,sw}P_{sw,BL,h}+\Psi X_{p,w}P_{w,BL,h})b$ and the net sectional stresses, resulting from the global bending load, is:

$$\sigma_{global}=(X_{m,sw}M_{sw,BL,h}+\Psi X_{m,w}P_{w,BL,h})/W_b. \tag{27}$$

σ_u is the ultimate stress capacity with a model uncertainty factor X_u, which is assumed to be described by the Normal probability density function, $N_{x,u}(1.05,0.1)$.

The model uncertainty factor $X_{m,w}$ accounts for the uncertainties in the wave induced vertical bending moment calculation. Resulting in $X_{m,w}\sim N_{x,m,w}(1,0.1)$ and the model uncertainty factor with respect to the still water load is $X_{m,sw}\sim N_{x,m,sw}(1,0.1)$ and with respect to the local pressure load are modelled by $X_{p,sw}\sim N_{p,sw}(1,0.1)$ and $X_{p,w}\sim N_{p,w}(0.95,0.095)$.

The fraction of time spent in each load condition may be estimated based on the statistical analysis of the operational profile of the bulk carrier ship. The assumed operational profile here is a full load, $p_{FL}=0.5$, ballast load, $p_{BL}=0.35$. The vertical wave-induced bending moment is in sagging in the full loading condition and in hogging in ballast and partial loading conditions. The still water bending moment is in sagging in full loading condition and in hogging in ballast and partial loading conditions. The ballast loading case is used in the present analysis since it transmits a compressive load to the stiffened plate at the bottom of the ship.

The still water bending moment is fitted to the Normal distribution. The regression Eqn define the statistical descriptors of the still water bending moment as a function of the length of the ship, W= (DWT/Full load) as proposed in [14, 15] and the loads are taken as prescribed by the Classification Societies Rules [3].

The 5% confidence level value of the ultimate bending moment $M_u^{5\%}=M_u^c$ is calculated by MARS2000 software and it is assumed that COV equals to 0.08 and it is fitted to the Lognormal probability density function:

$$f_{Mu}=\frac{1}{M_u\sigma_{Mu}\sqrt{2\pi}}e^{-\frac{(ln(M_u)-\mu_{Mu})}{2\sigma_{Mu}^2}} \tag{28}$$

$$\sigma_{Mu}=\sqrt{\ln(COV^2+1)} \tag{29}$$

$$\mu_{M_u}: F_{M_u}^{-1}(0.05,\mu_{M_u},\sigma_{M_u})=M_u^{5\%} \tag{30}$$

The ultimate bending moment statistical descriptors are given in Table 6.

Table 6 Statistical descriptors of ultimate bending moments

Load Conditions	Distribution	$Mean_{Msu}$	$StDev_{su}$	5%
$M_u(sag)$	Lognormal	9.699	0.08	14289
$M_u(hog)$	Lognormal	9.648	0.08	13578

Table7 Wave-induced dynamic pressure statistical descriptors (Gumbel distribution)

Load conditions	Fraction of time	n, cycles	α, MN.m	β, MN.m
FL(sag)	0.5	1971000	0.0248	0.00269
BL(hog)	0.35	1379700	0.0242	0.00268

Table 8 Wave-induced vertical bending moment, statistical descriptors (Gumbel distribution)

Load conditions	Fraction of time	n, cycles	α, MN.m	β, MN.m
FL(sag)	0.5	1971000	3481.8	378.0
BL(hog)	0.35	1379700	3115.3	345.5

The Gumbel distribution, for the extreme values of the vertical wave-induced bending moment, over the reference period T_r is derived based on the shape, h and scale, q factors of the Weibull distribution function as [16]:

$$\alpha_m = q(ln(n))^h \tag{31}$$

$$\beta_m = \frac{q}{h}(ln(n))^{(1-h)/h} \tag{32}$$

where α_m and β_m are the parameters of the Gumbel distribution, n is the mean number of load cycles expected over the reference time period T_r for a given mean value wave period T_w. It is assumed here that $T_r = 1$ year and $T_w = 8$ sec. The mean number of load cycles n is calculated as:

$$n = \frac{pT_r(365)(24)(3600)}{T_w} \tag{33}$$

where p is the partial time in which the ship is in seagoing conditions (full, ballast, partial loads)

The Gumbel distribution function is described as:

$$F_{Mw} = exp\left\{-exp\left(-\frac{M_{w,e}-\alpha_m}{\beta_m}\right)\right\} \tag{34}$$

where $M_{W,e}$ is a random variable that represents the extreme value of the vertical wave-induced bending moment over the reference time period, T_r.

The selected target ship is a bulk carrier larger than Panamax with 175,000 tones. For simplifying the calculation, the Alternate conditioned the Homogenous condition are catalogued into the full load condition. That is Full load condition: $p_1 = 0.5$;Ballast condition: $p_1 = 0.35$.

The wave-induced vertical bending moment and local dynamic pressure statistical descriptors are given in Table 7 and Table 8.

The still water bending moment is fitted to a Normal distribution. Regression Eqn defines the statistical descriptors of the still water bending moment as a function of length, *L* and dead-weight ratio, *W*= (DWT/Full load), which coefficients are given in Table 9 and the calculated mean and standard deviation of still water bending moment are listed in Table 10.

Table 9 Mean value and standard deviation of still water bending moment

	FL(sag)	BL(hog)
$\mathrm{Mean}(M_{SW,max})$	-24.846	49.074
$\mathrm{StDev}(M_{SW,max})$	21.215	26.115

$$\mathrm{Mean}(M_{SW}) = \frac{\mathrm{Mean}(M_{SW,max})M_{SW,CS}}{100} \tag{35}$$

$$\mathrm{StDev}(M_{SW}) = \frac{\mathrm{StDev}(M_{SW,max})M_{SW,CS}}{100} \tag{36}$$

Table 10 Still water bending moment

Load conditions	W=DWT/ Full Load	Distribution	Mean, (MN.m)	StDev, (MN.m)
FL (Sagging)	0.9	Normal	968.939	827.338
BL (Hogging)	0.2	Normal	2186.468	1163.541

The statistical descriptions of the uncertainty coefficients involved in the limit state function are assumed and listed in Table 11.

Table 11 Uncertainty coefficients

Uncertainty factors	Distribution	Mean	StDev	COV
X_u	Normal	1.05	0.1	0.1
X_{SW}	Normal	1.00	0.1	0.1
X_W	Normal	1.00	0.1	0.1
X_S	Normal	1.00	0.1	0.1

Where denotes the normal distribution function and the first and second indicator inside of the brackets refer to the mean value and standard deviation respectively.

3.5 *Analysis*

3.5.1 *Multi-objective optimisation*

The Pareto frontier [17] is employed here allowing for the optimisation of the three criterion, as they are defined in the present study as the minimisation of net sectional area, displacement and the fatigue damage factor D, verifying all trade-offs among the optimal design solutions of the three criterion.

The multi-objective optimisation was performed and the solution contains a series of optimal results, each of them includes the five design variables which determine the shape and area of the stiffened plate with the corresponding results of the three objective functions which are a sectional area, displacement at the middle of the span and the fatigue damage factor D.

Figure 4 shows the minimisation of the two objective functions, F_1 (net sectional area) and F_3 (fatigue damage) simultaneously. Figure 5 shows the minimization of the two objective functions, F_1 (net sectional area) and F_2 (displacement) simultaneously.

Figure 4 indicates that the Pareto optimal frontier, whereby any improvement concerning F_1 comes at the bigger value of F_2. Each design solution, allocated at that frontier represents unique design solution parameters. The Pareto optimal solution collected here 100 optimal design solutions that are going to be verified with respect to the target reliability in the next section, leading to an additional constraint in the optimization process.

After that the points that do not meet the regulations were deleted, one can move on to the next step, the reliability design.

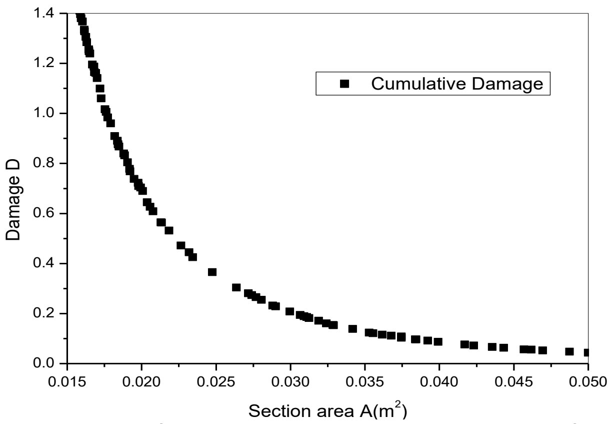

Figure 1 Pareto frontier solution:-net section area vs fatigue damage

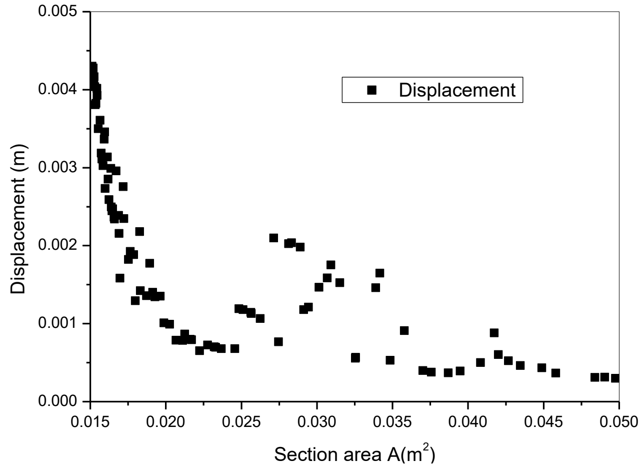

Figure 2 Pareto frontier solution: net section area vs displacement

3.5.2 *Reliability-based design optimisation*

The reliability analysis is incorporated into the optimisation procedure, which is referred to here as reliability-based design optimisation, RBDO. The statistical nature of the constraints and design problems are defined in the objective function including the probabilistic constraints. The probabilistic constraints can specify the required reliability target level.

The reliability is performed based on the FORM [18, 19], and all random variables are considered as non-correlated ones. Applying FORM as a decision tool, the estimated probability of failure needs to be compared to an accepted target level. The target levels depend on different factors as reported in [20]. The target level adapted here, which may result in a redundant structure in $P_f = 10^{-3}$ ($\beta = 3.09$) for less serious and $P_f = 10^{-4}$ ($\beta = 3.71$) for serious consequences of failure values of the acceptable annual probability of failure [11].

During the buckling check step, the input values of the random variables, which describe the two loading conditions were taken into consideration, and so the two kinds of results were obtained. The Beta index of the buckling check is the combination of the two states using the fraction of time of the load condition of the bulk carrier as the weighting coefficient. After that, the result of the buckling check is combined with the results obtained by fatigue check again. At this point, the probability of the two outcomes is assumed for both as 0.5.

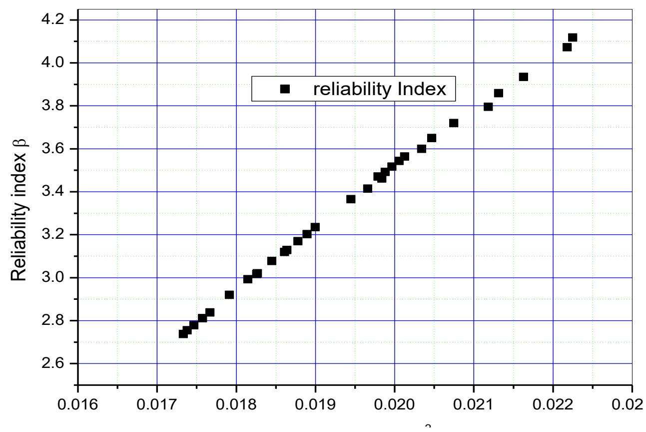

Figure 3 Beta index as a function of the net sectional area

The final Beta index and its corresponding objective function values were calculated. The reliability index β, as a function of the net section area, is shown in Figure 6. The range of the Beta index of all design solutions at the Pareto frontier is from 2.737 to 4.11.

The design solution n° 6, $\beta = 3.72$ fits all constrains of the two objective functions and the required safety target level, as defined to be here, $\beta_{target} = 3.7$.

The optimization result of the stiffened plate with reliability index 3.72 is that t_p = 0.012 m (12 mm), h_w=0.496m(496mm), t_w = 0.0173 m (17 mm), b_f = 0.1526 m (153 mm), t_f = 0.012 m (12 mm), the section area equals to 0.02075 (m^2).

Comparison with the original design section area = 0.0225 m^2, the optimised section area is reduced by 8%.

4 CONCLUSIONS

The objective of this work was to perform a multi-objective nonlinear structural optimisation of a stiffened plate subjected to combined stochastic compressive loads accounting for the ultimate strength and reliability based constraints in the design. The solution of the three-objective structural responses, in minimising the weight, structural displacement and fatigue damage, was considered. The Pareto frontier solution was used to define the feasible surface solution of the design variables.

The reliability, index which defines the shortest distance from the origin to the limit-state boundary, was employed to identify the topology of the stiffened plate as a part of the Pareto frontier solution. Comparing with the original section area, the optimised section area is reduced by 8%. The presented methodology is flexible and demonstrated an excellent capacity to be used in the structural design of complex systems.

REFERENCE

[1] Guedes Soares, C. and Soreide, T. H., 1983, "Behaviour and Design of Stiffened Plates Under Predominantly Compressive Loads", *International Shipbuilding Progress*, 30, (341), pp. 13-27.

[2] Garbatov, Y. and Georgiev, P. "Optimal design of stiffened plate subjected to combined stochastic loads". *In: Progress in the Analysis and Design of Marine Structures*. C. Guedes Soares and Y. Garbatov, editors. London: Taylor & Francis Group, 2017, pp. 243-252.

[3] IACS. "Common Structural Rules for Bulk Carriers and Oil Tankers". London: International Association of Classification Societies, 2015.

[4] Garbatov, Y. and Guedes Soares, C., 1998, "Fatigue Reliability of Maintained Welded Joints in the Side Shell of Tankers", *Journal of Offshore Mechanics and Arctic Engineering*, 120, (1), p. 2.

[5] Garbatov, Y. and Guedes Soares, C., 2002, "Bayesian Updating in the Reliability Assessment of Maintained Floating Structures", *Journal of Offshore Mechanics and Arctic Engineering*, 124, (3), p. 139.

[6] Guedes Soares, C. and Teixeira, A. P., 2000, "Structural reliability of two bulk carrier designs", *Marine Structures*, 13, (2), pp. 107-128.

[7] Teixeira, A. P., Guedes Soares, C. and Wang, G., 2012, "Probabilistic modelling of the ultimate strength of ship plates with non-uniform corrosion", *Journal of Marine Science and Technology*, 18, (1), pp. 115-132.

[8] Horn, J., Nafpliotis, N. and Goldberg, D., 1994, "A niched Pareto genetic algorithm for multiobjective optimisation", *IEEE World Congress on Computational Intelligence*, Vol. 1, pp. 82-87.

[9] Deb, K., Pratap, A., Agrawal, S. and Meyarivan, T., 2002, "A Fast and Elitist Multi-objective Genetic Algorithm: NSGA-II", *IEEE Transactions on Evolutionary Computation*, 6, (2), pp. 182-197.

[10] MARS2000, 2011, *Bureau Veritas, Rules for the Classification of Ships and IACS Common Structural Rules for Bulk Carriers and Tankers*: Bureau Veritas.

[11] DNV. "Structural Reliability Analysis of Marine Structures". In: Classification notes No 30.6 Hovik: DnV, 1992.

[12] Guedes Soares, C. and Moan, T. "Statistical Analysis of Still - Water Bending Moments and Shear Forces on Tankers and Bulk Carriers". In: Norwegian Maritime Research, Vol. 10, 1982, pp. 33-47.

[13] Guedes Soares, C. and Gordo, J. M., 1996, "Compressive Strength of Rectangular Plates Under Biaxial Load and Lateral Pressure", *Thin-Walled Structures*, 24, pp. 231-259.

[14] Guedes Soares, C. and Moan, T., 1988, "Statistical Analysis of Still-Water Load. Effects in Ship Structures", *Transactions of the Society of Naval Architects and Marine Engineers (SNAME)*,, 96, pp. 129-156.

[15] Guedes Soares, C., 1990, "Stochastic Modelling of Maximum Still-Water Load Effects in Ship Structures", *Journal of Ship Research*, 34, pp. 199-205.

[16] Guedes Soares, C., Dogliani, M., Ostergaard, C., Parmentier, G. and Pedersen, P. T., 1996, "Reliability Based Ship Structural Design", *Transactions of the Society of Naval Architects and Marine Engineers (SNAME)*, 104, pp. 359-389.

[17] Komuro, R., Ford, E. D. and Reynolds, J. H., 2006, "The use of multi-criteria assessment in developing a process model", *Ecological Modelling*, 197, (3-4), pp. 320-330.

[18] Hasofer, A. M. and Lind, N. C., 1974, "An exact and invariant first-order reliability format", *Journal of Engineering Mechanics Division, ASUE*, 100, pp. 111-121.

[19] Hasofer, A. M. and Lind, N. C., 1974, "Exact and invariant second-moment code format", *Journal of the Engineering Mechanics Division*, 100, (1), pp. 111-121.

[20] Moan, T. "Target levels for structural reliability and risk analyses of offshore structures". *In: Risk and reliability in marine technology*. G. Soares, editor. Rotterdam: A.A. Balkema, 1998.